4-D segmentation and normalization of 3He MR images for intra-subject assessment of ventilated lung volumes

Benjamin Contrella[a], Nicholas J. Tustison[a], Talissa A. Altes[a], Brian B. Avants[b], John P. Mugler III[a], Eduard E. de Lange[a]

[a]University of Virginia
[b]University of Pennsylvania

ABSTRACT

Although 3He MRI permits compelling visualization of the pulmonary air spaces, quantitation of absolute ventilation is difficult due to confounds such as field inhomogeneity and relative intensity differences between image acquisition---the latter complicating longitudinal investigations of ventilation variation with respiratory alterations. To address these potential difficulties, we present a 4-D segmentation and normalization approach for intra-subject quantitative analysis of lung hyperpolarized 3He MRI. After normalization, which combines bias correction and relative intensity scaling between longitudinal data, partitioning of the lung volume time series is performed by iterating between modeling of the combined intensity histogram as a Gaussian mixture model and modulating the spatial heterogeneity tissue class assignments through Markov random field modeling. Evaluation of the algorithm was retrospectively applied to a cohort of 10 asthmatics between 19-25 years old in which spirometry and 3He MR ventilation images were acquired both before and after respiratory exacerbation by a bronchoconstricting agent (methacholine). Acquisition was repeated under the same conditions from 7 to 467 days (mean ± standard deviation: 185 ± 37.2) later. Several techniques were evaluated for matching intensities between the pre and post-methacholine images with the 95th percentile value histogram matching demonstrating superior correlations with spirometry measures. Subsequent analysis evaluated segmentation parameters for assessing ventilation change in this cohort. Current findings also support previous research that areas of poor ventilation in response to bronchoconstriction are relatively consistent over time.

Keywords: bias correction, hyperpolarized 3He, lung, segmentation

1. INTRODUCTION

Prior to the last decade, little was known about the temporal and spatial distribution of ventilation defects in the lungs of asthmatics. Spirometry was used and continues to be used to provide valuable insight into the vasoconstriction occurring in the bronchi and bronchioles of the lungs of asthmatics. It is used diagnostically to obtain information on total airflow volume and rate in the lungs of patients with pulmonary difficulties including asthma, but it is unable to provide higher resolution detail on areas of the lung that remained well ventilated during an asthma exacerbation as compared to those that became poorly ventilated (de Lange et al 2006). This promoted questions such as whether poorly ventilated areas of lung tissue were consistent over time, whether they appeared in the same areas of the lung during bronchoconstriction, and if constriction occurred in a lobar distribution or in scattered bronchioles.

In recent years, hyperpolarized helium-3 MR lung ventilation imaging has been used to gain insight into the temporal and spatial distribution of poorly ventilated areas of lung parenchymal tissue (de Lange et al 2006). Use of 3He as an inhaled contrast agent allows for visualization of ventilated air spaces and therefore identification of ventilation defects, and its use in quantifying regions of poor ventilation seems to be the top performing factor in differentiating between the clinical diagnoses of asthma and normal lungs (de Lange et al 2007, Tustison et al 2010b). Use of this technology offers numerous advantages over spirometry. While spirometry is limited to drawing generalizations about the lungs as a whole, 3He MRI images provide more detailed information on the degree and location of ventilation defects throughout the lungs. Information from this imaging modality is of value in that it could give insight into processes in the lungs that could not be learned from spirometry alone and provide answers to longstanding questions about ventilation defects in

Medical Imaging 2012: Biomedical Applications in Molecular, Structural, and Functional Imaging, edited by Robert C. Molthen, John B. Weaver, Proc. of SPIE Vol. 8317, 83171D · © 2012 SPIE · CCC code: 1605-7422/12/$18
doi: 10.1117/12.911032

the lungs of asthmatics such as correlation between asthma severity and distribution of defects and consistency in the location of defects during bronchoconstriction.

In past usage, a major drawback of helium-3 MR imaging was that it was a time consuming process for radiologists to study the images and score areas that qualify as defects (Tustison et al 2011). Even when studied carefully, a study has shown that the sensitivity of experienced radiologists is somewhat limited (de Lange et al 2006). This problem is mitigated by automated segmentation methods, such as Atropos, for ventilation-based partitioning of lungs in hyperpolarized 3He MR images. Atropos utilizes conventional Gaussian mixture modeling and non-parametric approaches for histogram fitting as well as prior-based strategies including template and/or Markov random field priors (Tustison et al 2011, Avants et al 2011). The result is an algorithm that can analyze images much faster than traditional methods with improved sensitivity and specificity (Tustison et al 2011) in spite of algorithmic confounds such as field inhomogeneity and relative intensity differences between image acquisitions---the latter complicating longitudinal investigations of ventilation variation with respiratory alterations. In this work, we describe the development and evaluation of normalization and segmentation strategies for intra-subject differentiation of ventilated and non-ventilated lung parenchyma using Atropos on hyperpolarized 3He MRI data. We then apply this method retrospectively to data from a study of asthmatics who underwent a methacholine challenge at two timepoints to assess the method and evaluate if defects appeared in the same area of the lung.

2. METHODS

2.1 Image and spirometry acquisition

Retrospective analysis was applied to the data described in (de Lange et al 2007). 10 subjects between the ages of 19 and 25 years (mean ± standard deviation: 20.9 ± 1.6) were screened for mild-to-moderate asthma. Each subject underwent 2 respiratory (methacholine) challenges between 7 and 467 days (mean ± standard deviation: 185 ± 37.2). Methacholine is a bronchoconstricting agent, so its use in the study was designed to induce the appearance of ventilation defects resembling those that would be seen in an acute asthma exacerbation. 3He axial MRI spanning the entire lung (19-28 10 mm slices) were acquired immediately before and after the administration of methacholine. Spirometry measures were also acquired at baseline each day and 2 minutes post-methacholine administration. Further details regarding the image acquisition and spirometry can be gleaned from (de Lange et al 2007).

2.2 Image Analysis

We recently proposed a ventilation-based segmentation pipeline for parcellation of lung volumes into ventilated and non-ventilated regions which demonstrated superior specificity/sensitivity when compared with human raters (Tustison et al 2011). The two major components of the proposed workflow are N4 bias correction (Tustison et al 2010a) for removing the low-frequency intensity variation artifact associated with the inhomogeneity field and a 4-D Bayesian segmentation strategy (Tustison et al 2011) incorporating many elements common to brain segmentation (Avants et al 2011). After the N4 bias correction was performed but before the segmentation, images were further adjusted to remove the vasculature from being recognized by the segmentation algorithm. The 3He images display areas of ventilation as bright and areas without ventilation as dark, so the larger vessels, into which the helium does not diffuse, appear dark and can be mistaken for poorly ventilated parenchymal tissue. This could distort the percentage of tissue determined as poorly ventilated both before and after the methacholine, so it is desirable that the vasculature be excluded.

Separating the vasculature from the parenchymal tissue was a multistep process, and images from different steps are shown in Figure 1. A mask was first created for each 3He image (Figure 1b) via registration of a standardized mask represeneting an average lung (Avants et al 2010). Such a mask is necessary prior to running the segmentation because of the difficulties in distinguishing unventilated lung tissue from background on the 3He MR images. The 3He image was then divided from a 3D image of 15-28 slices into 15-28 individual 2D slices (a sample slice is shown in Figure 1a) for Hessian-based filtering of the lungs to enhance the airways for subsequent mask removal (Frangi et al 1998). Note that individual 2-D slice handling was necessary due to voxel anisotropy in the through-plane direction.

To improve the accuracy of the vasculature segmentation, we limit segmentation to the area around the hilum of the lung. As almost all of the vasculature large enough to appear on the 3He MRI is concentrated around the hilum, most of

the area marked as vasculature outside that area was considered likely to be ventilation defects that resemble vasculature. The hilum mask was propagated to each individual subject as it was defined on the average mask previously described. (Figure 1d). This mask was overlaid with the vasculature mask to create a mask including only the vasculature in the hilum. Finally, the mask was overlaid with the original mask to create a mask encompassing the lungs except for the vasculature in the hilum (Figure 1e).

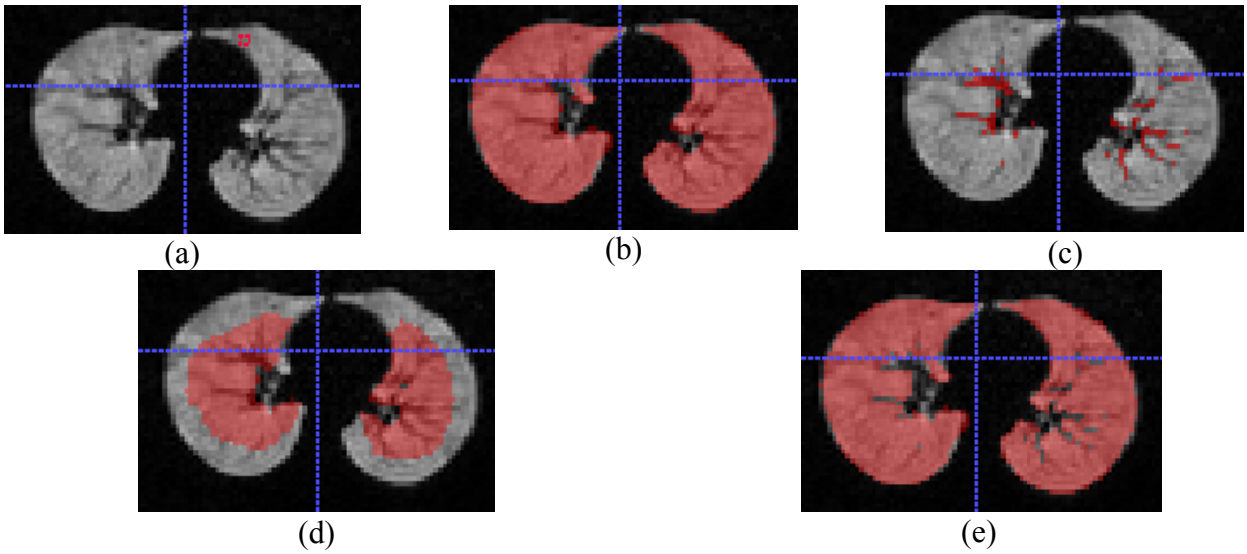

Figure 1. Editing of 3He MR scan for Subject 4. (a) Slice of the image without mask. (b) Same slice of image with mask. (c) Vasculature from image as identified by HessianBasedFeatures script (d) Small mask used to limit vasculature delineation to area where vasculature is often found. (e) Mask with areas of vasculature found within the area of figure 3d subtracted out.

The final mask was then segmented using the second component of the proposed workflow. The basic intuition behind this strategy is an iterative optimization between Gaussian mixture modeling (GMM) of the intensity histogram describing the intensity values of 4-D data coupled with a Markov random field (MRF) model for incorporating tissue classification smoothing between neighboring voxels. Although the spatial component of the MRF model is useful for mitigating the effects of noise within a single 3-D volume, we minimized longitudinal smoothing of the MRF model since a) the images were not registered and b) longitudinal smoothing would bias the effects of the pre- and post- aspects of the analysis quantifying the transience/permanency of ventilation defects across time. Towards the latter analysis, the binary lungs masks from each of the 4 time points were used to create a single unbiased mean mask template for each subject (Avants et al 2010). The segmentation from each of the 4 time points was then warped to the template space where voxelwise comparisons could be performed (see Figure 2).

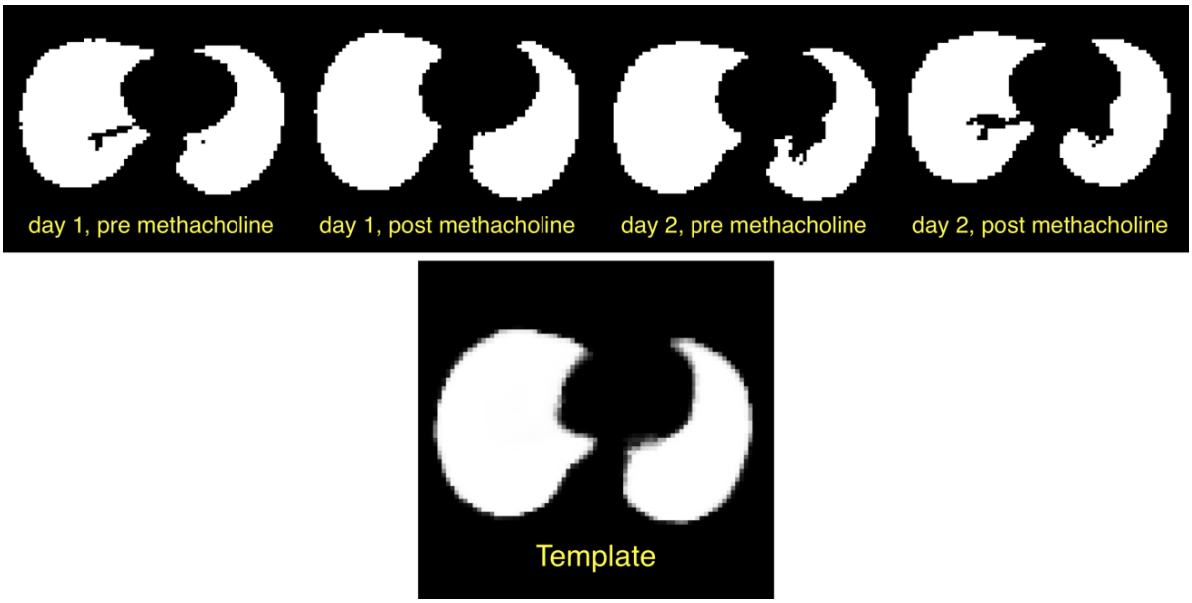

Figure 2. Top row: mid-axial slice masks from Subject 5 derived from the 3He MR images taken at pre- and post-Administration of methacholine. Bottom row: mid-axial slice of the average shape template created from the volumetric image masks.

3. RESULTS

Data acquisition aimed to determine which method of data normalization most accurately adjusts the images and assess the transience of defects between acquisitions. Toward the former goal, correlation values between each normalization and spirometry and radiologist analysis were calculated and compared. A high degree of correlation suggests that the normalization method in conjunction with the segmentation algorithm is effective in differentiating defects. Toward the latter goal, Jaccard overlap measures were used to quantify the defects that remained in the same location between the two days of acquisition.

Section 3.1 Intensity histogram normalization

We evaluated different intensity histogram normalization techniques by performing segmentation on the four time points for each subject after bias correction and determining the r^2 correlation value with different spirometry values acquired at each time point. This allowed us to determine if our 4-D segmentation approach was superior to separate segmentation of the 3-D volumes and if intensity histogram normalization (which included both 95th percentile matching and dynamic histogram warping (Cox et al 1995)) was superior to no histogram normalization. It was found that no histogram matching on the 4-D segmentation performed worst of all the possible experimental permutations with practically no correlation between spirometry and the segmentation results (r^2_{FEV1}=0.01, $r^2_{FEV1\%pred}$=0.02, and $r^2_{FEF25-75\%}$=0.01). However, 4-D segmentation of the histogram matched images based on the 95th percentile value was most correlated with spirometry (For day1, r^2_{FEV1}=0.86, $r^2_{FEV1\%pred}$=0.86, and $r^2_{FEF25-75\%}$=0.849 ; for day 2, r^2_{FEV1}=0.41, $r^2_{FEV1\%pred}$=0.41, and $r^2_{FEF25-75\%}$=0.55) exceeding all other scenarios by at least 0.1.

Figure 3. Pre- (left) and post-methacholine (right) segmentation for Subject 8 using the method proposed.

Correlation was also calculated between the number of ventilation defects as determined by radiologist review of the uncorrected images and the defects found in each of the segmentation approaches tested. The 4-D segmentation with the histogram matched images based on 95th percentile values had the highest correlation, with r values of 0.8540 and 0.8621 for days 1 and 2 respectively. Correlation values for each of the segmentation methods are given in Table 1.

Table 1. Correlation values between % change in parenchyma with ventilation defect before as compared to after methacholine as determined by each of the segmentation methods and spirometry or radiologist assessment values

	ΔFEV1%	**ΔFEF$_{25-75\%}$**	**Δ Defects Identified by radiologist**
4D 95th Percentile:Day1	-0.8556	-0.8490	0.8540
Day2	-0.4046	-0.5549	0.8621
3D 95th Percentile:Day1	-0.8439	-0.8832	0.879
Day2	-0.422	-0.541	0.765
4D Hist. Matched:Day1	-0.7746	-0.7558	0.7707
Day2	-0.7030	-0.6024	0.3390
3D Hist. Matched:Day1	-0.6299	-0.6959	0.7346
Day2	-0.5426	-0.3394	0.560

Section 3.2 Assessment of defect transience

To determine how much the ventilation defects changed between acquisition days, we calculated the union, or Jaccard, overlap between the ventilation defect segmentations between the two pre-methatcholine time points and between the two post-methacholine time points. These ratios are shown in Table 2. We also performed a paired t-test ($\alpha = 0.05$) to determine if the ratios were greater before or after each subject's methacholine challenge with results indicating that overlap was greater for the post-methacholine images.

Table 2. Jaccard overlap measures comparing the two time points after registration of segmentation results to the template. The percent overlap is increased with the post-methacholine data (p-value = 0.02, $\alpha = 0.05$, two-tailed paired t-test).

Subject	**Jaccard (Pre Methacholine)**	**Jaccard (Post Methacholine)**
Subject 1	0.229799	0.376712
Subject 2	0.153691	0.410184
Subject 3	0.218949	0.365444
Subject 4	0.320826	0.257199
Subject 5	0.291062	0.268575
Subject 6	0.236266	0.348313
Subject 7	0.23884	0.303008
Subject 8	0.324092	0.294598
Subject 9	0.151801	0.314601
Subject 10	0.23772	0.401973

4. CONCLUSIONS

A 4-D segmentation and normalization approach to quantifying ventilation defects in hyperpolarized 3He MRI was described. We evaluated different permutations of longitudinal segmentations and it was shown, based on correlations with spirometry, that 4-D segmentation where the longitudinal data has been histogram-matched based on the 95th percentile value provided superior results. This was also demonstrated using data acquired pre- and post-administration of methacholine in 10 asthmatic subjects.

This work presents possibilities for future work in the processing and evaluation of 3He MR images, both in terms of applying the method to other studies and in terms of further refining the method for improved accuracy. Toward the latter goal, we have recently worked with an adjusted pipeline wherein the actual bias corrected images are warped rather than warping masks. In this strategy, the image post-methacholine administration would be warped to fit in the same set of coordinates as the image from before methacholine administration, then both images can be segmented using either a 3D method with histogram matching at the 95th percentile or a 4D method with histogram matching at the 95th percentile. The advantage of this method may be to reduce the noise in small poorly ventilated areas that could reduce the overall accuracy by falsely elevating the percentage of defects that are at different locations before and after methacholine administration.

We have also identified several other studies that this method could be applied to, both to further test its effectiveness and to gain further insight into the response of the lungs to different stimuli. The first study was a repeatability study wherein two 3He MR images of a subject were taken fifteen minutes apart with no intervention between imaging. Analysis of the difference in spatial distribution of defects between the two images, specifically the overlap, could provide insight into how accurate the current method is in identifying defects (assuming that the location of defects would change minimally in the fifteen minutes between images). Preliminary results from analysis of this study using a version of the new method proposed above (warping of the images) indicates a more than 80% overlap in ventilated/non-ventilated tissue between the first and second images.

Another study to which this method has been applied involves the analysis of images taken at baseline, immediately after administration of a vasodilator, albuterol, and around four hours after the administration of the albuterol. We analyzed the overlap in defects between the baseline and the time point immediately after albuterol administration and between the baseline and the time point four hours after albuterol administration. Early results from analysis of this study would seem to indicate both an absolute decrease in the percent of unventilated tissue after administration of the albuterol (as would be expected) as well as a decrease in the percent of defects present prior to the albuterol that remained in the same location after the albuterol. This decrease, which continues in the time point 4 hours after albuterol administration, could be due to improvements from the albuterol manifesting hours after administration or a shift in the defects with time. Given the short time scale on which the all the images were taken and on the decrease in poorly ventilated tissue four hours after the albuterol compared to immediately after albuterol administration, the former seems more likely. However, variations are certainly well within expected margin of error.

REFERENCES

[1] Avants BB, Tustison NJ, Wu J, Cook PA, Gee JC, "An Open Source Multivariate Framework for *n*-Tissue Segmentation with Evaluation on Public Data", Neuroinformatics 2011, epub ahead of print.

[2] Avants BB, Yushkevich P, Pluta J, Minkoff D, Korczykowski M, Detre J, Gee JC, "The optimal template effect in hippocampus studies of diseased populations," Neuroimage, 49(3), 2457 (2011).

[3] Cox, IJ and Hingorani, SL, "Dynamic histogram warping of image pairs for constant image brightness," International Conference of Image Processing- Proceedings, Vols I-III, B366 - B369 (1995).

[4] de Lange EE, Altes TA and Patrie JP *et al.*, "Evaluation of asthma with hyperpolarized helium-3 MRI: Correlation with clinical severity and spirometry," Chest, 130, 1055–1062 (2006).

[5] de Lange EE, Altes TA, Patrie JT, Parmar J, Brookeman JR, Mugler JP III, Platts-Mills TA., "The variability of regional airflow obstruction within the lungs of patients with asthma: assessment with hyperpolarized helium-3 magnetic resonance imaging," J Allergy Clin Immunol, 119, 1072–1078 (2007).

[6] Frangi A, Niessen W, Vincken K, Viergever M, "Multiscale vessel enhancement filtering," Proceedings of the Medical Image Computing and Computer Assisted Intervention Society, 130–137 (1998).

[7] Tustison NJ, Avants BB, Cook P, Egan A, Chen Y, Yushkevich P, Gee JC, "N4ITK: Improved N3 bias correction," IEEE Trans Med Imaging, 29, 1310-1320 (2010).
[8] Tustison, NJ, Altes, TA, Song, G, de Lange, EE, Mugler, JP, Gee, JC, "Feature analysis of hyperpolarized helium-3 pulmonary MRI: A study of asthmatics versus nonasthmatics," Magnetic Resonance in Medicine, 63, 1448–1455 (2010).
[9] Tustison NJ, Avants BB, Flors L, Altes TA, de Lange EE, Mugler JP, Gee JC, "Ventilation-Based Segmentation of the Lungs Using Hyperpolarized 3He MRI," JMRI, 34(4), 831-838 (2011).